



# Estimating strength parameters of Lower Gondwana coal measure rocks under dry and saturated conditions

TABISH RAHMAN and KRIPAMOY SARKAR\*

Department of Applied Geology, Indian Institute of Technology (Indian School of Mines) Dhanbad, Dhanbad 826 004, Jharkhand, India.

\*Corresponding author. e-mail: kripamoy.sarkar@gmail.com

MS received 26 July 2021; revised 23 February 2022; accepted 6 March 2022

Coal mining operations below the water table of surface and underground mines are common. Therefore, a better understanding of rock behaviour in dry and water-saturated conditions is critical in rock engineering projects. In this paper, Lower Gondwana coal measure rock (sandstone and shale) samples have been collected from 10 different mines (eight collieries) in Jharia and Raniganj coalfield of Damodar basin, India. The strength parameters (uniaxial compressive strength (UCS) and Brazilian tensile strength (BTS)) primarily govern the design aspects in mining. These are the most common input parameters for any rock mass classification. Hence, changes in the strength parameters of coal measure rocks under dry and water-saturated conditions would adversely lead to the change in the rock mass classification of the rock. Moreover, the direct determination of strength parameters is expensive, time-consuming, field-inaccessible, laborious, destructive, and requires experienced labour, while an indirect method to estimate the strength parameters from ultrasonic pulse velocity (UPV) is cheap, easy, quick, field-accessible, non-destructive, and straightforward. The UPV, UCS, and BTS in dry conditions, density ( $\rho$ ), porosity ( $\phi$ ) and rock type information were used as input parameters for predicting the UPV, UCS and BTS in saturated conditions using simple regression (SR), multivariate regression (MR) and artificial neural network (ANN). The change in UPV, UCS and BTS from dry to saturated conditions were observed to be a function of the intrinsic properties ( $\rho$  and  $\phi$ ) of coal measure rocks. Finally, a comparative analysis between SR, ANN and MR was performed in a measured *vs.* predicted 1:1 scatter plot.

**Keywords.** Uniaxial compressive strength; Brazilian tensile strength; ultrasonic pulse velocity; simple regression; multivariate regression; artificial neural network.

## 1. Introduction

The coal measure rocks are essentially encountered during mining of coals in underground as well as open-cast mines of Lower Gondwana basins of India. When the mining is carried out, the rocks encountered are sometimes moderately or completely saturated or wet due to the percolation of water from the surface or essentially saturated with water when the mining is carried out below the

water table. So, the strength parameters determined under dry condition tends to be misleading for the saturated rocks encountered below the water table during mining operations. Hence, for safe mining and mine development, the characterisation of encountered rocks is essential in dry as well as saturated conditions. The direct determination of strength parameters is a very tough, expensive, field-inaccessible, destructive and time-consuming job, while estimation of strength

parameters using UPV is a simple, cheap, field-accessible, non-destructive, quick and easy method. Therefore, empirical correlations have been proposed between strength parameters and UPV of coal measure rocks under dry and saturated conditions so that the strength parameters can be estimated quickly and easily in both conditions. The relationship was also established with the strength parameters and intrinsic properties and change in UPV, UCS, and BTS ( $\Delta_{UPV}$ ,  $\Delta_{UCS}$ , and  $\Delta_{BTS}$ , respectively) and intrinsic properties.

Hawkins and McConnell (1992) observed the influence of moisture content on the UCS and deformability of 35 British sandstone types. They found that the UCS and deformability of sandstones reduced as the moisture content increased. Steiger and Leung (1990) stated the decrease in UCS of three types of shale samples in a saturated condition. Dyke and Dobereiner (1991) investigated the variation in UCS with changing moisture content and concluded that the weaker rocks are more sensitive to changes in moisture content. Vasarhelyi (2003) established a relationship between dry and saturated UCS and dry and saturated Young's modulus (both sec and tan). Lin *et al.* (2005) observed that inter-granular fractures exist in all dry sandstones, and the strength and stiffness reduce when the sandstones are wet. Vasconcelos *et al.* (2007) studied the mechanical and physical parameters of granites using indirect UPV tests and also proposed a correlation between dry and saturated UPV for a wide variety of granites. Torok and Vasarhelyi (2010) analysed Hungarian travertine rocks under air-dry and saturation conditions. They proposed correlations between UCS–UPV (dry and saturated),  $UPV_{dry}$ – $UPV_{sat}$ , UCS–density and porosity and  $UCS_{dry}$ – $UCS_{sat}$ . Karakul and Ulusay (2013) suggested correlations to predict the strength parameters of different rock types using UPV at different degrees of saturation.

Kahraman (2007) modelled a linear correlation between dry and wet UPV for different rock types with high  $R^2$  values. He also concluded that change in UPV is greater for rocks with porosity <1% and change in UPV is lower for rocks having porosity >1%. He also proposed regression equations for sedimentary, metamorphic and igneous rocks. Mashinskii (2009) experimentally studied the attenuation of frequency and strain amplitude of P- and S-wave in dry and saturated sandstone samples under the load of 20 MPa. He found that strain amplitude is inversely dependent on P-wave

attenuation in dry and S-wave attenuation in dry and saturated conditions, and P-wave attenuation in saturated conditions showed no dependence on strain amplitude. Many researchers have correlated the geomechanical properties of rocks in dry conditions with the UPV (Yasar and Erdogan 2004; Chary *et al.* 2006; Kilic and Teymen 2008; Sharma and Singh 2008; Altindag 2012; Azimian 2017; Rahman *et al.* 2020; Rahman and Sarkar 2021).

Artificial neural network (ANN) has been widely used as a supervised soft-computing tool to estimate different physico-mechanical parameters in the previous studies. Ghabousi *et al.* (1991) used the backpropagation neural network to model the behaviour of concrete under plane stress and uniaxial cycle load conditions. Singh *et al.* (2001) predicted the strength properties of different types of schist rock from the textural properties using the ANN. Sharma *et al.* (2017) used the neural network and neuro-fuzzy approach to predict the UCS from three geomechanical input properties, namely, slake durability index, density and UPV.

In this paper, 14 types of sandstones and 13 types of shale samples from eight collieries of Jharia and Raniganj coalfields have been studied under dry and saturated conditions. The sandstone and shale samples have been categorised into 14 and 13 types, respectively on the basis of obtained geomechanical (UCS, BTS), physical ( $\phi$  and  $\rho$ ), ultrasonic pulse velocity parameters and the locations from which the samples have been collected. The geomechanical properties such as UCS and BTS have been correlated with the UPV under dry and saturated conditions. The relationships between these parameters have been studied for both rock types (sandstone and shale). The changes in the strength parameters and UPV were also assessed, and relationships have been proposed. ANN, which is an advanced modelling technique, has been used to predict the strength parameters under saturated conditions.

## 2. Study area

The study area is located in the energy storehouse of India. The Jharia and Raniganj coalfields are the most prolific coal-bearing regions sited in the state of Jharkhand and West Bengal, respectively (figure 1). A total number of 14 types of sandstone and 13 types of shale samples were used in the present study from five coalfield areas (Satgram,

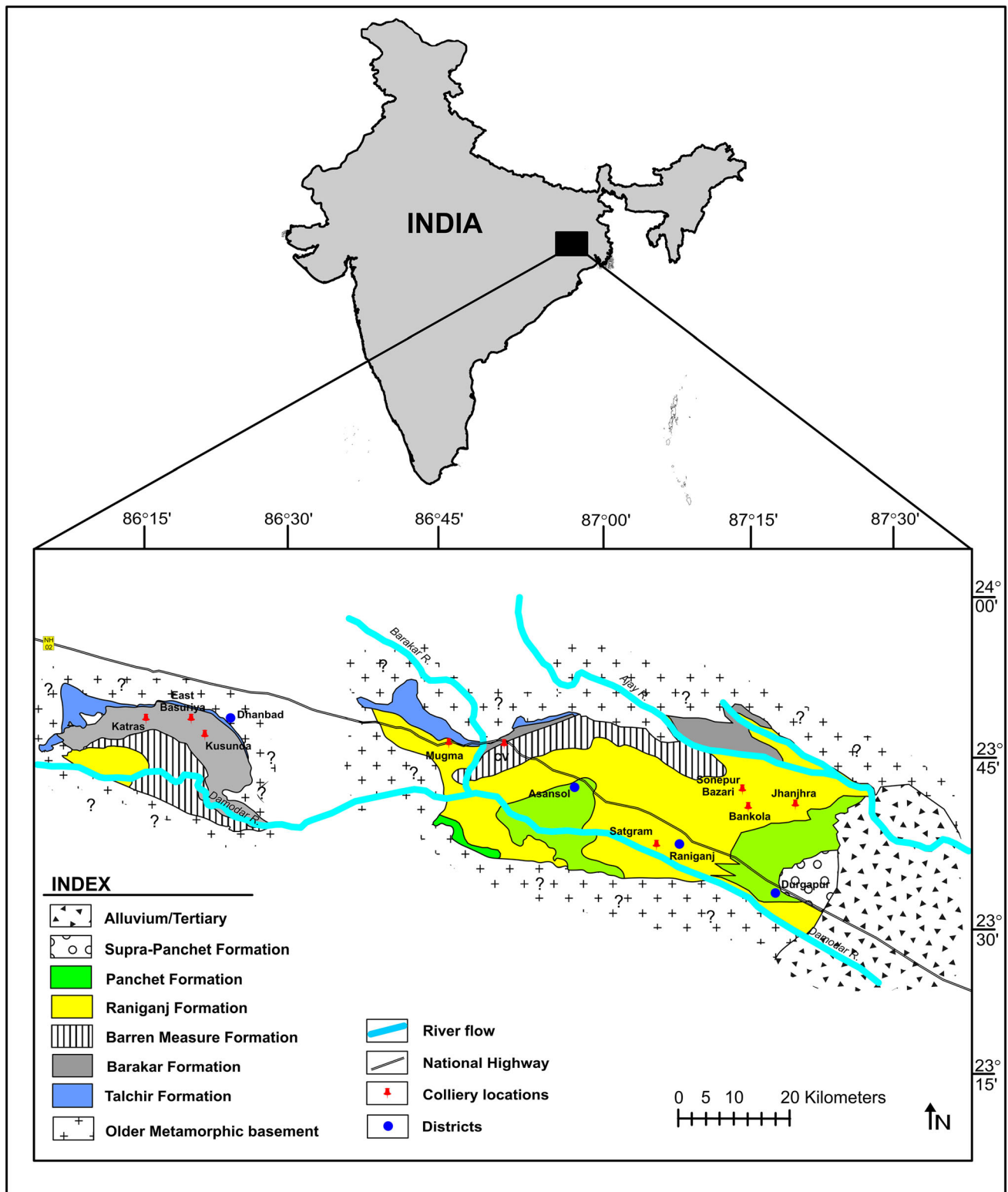


Figure 1. Geological map showing the distribution of colliery areas under study (after Fox 1930 and GSI 2003).

Mugma, Sonapur Bazari, Bankola and Jhanjhra area) of Raniganj coalfields under ECL (Eastern Coalfields Ltd.) and two coalfield areas of Jharia coalfields (Katras and Kusunda area) and CV area

of Damagoria coalfields under BCCL (Bharat Coking Coal Ltd.) (table 1).

The coal measure rocks range in age from Upper Carboniferous to Lower Triassic (Vaidyanadhan

Table 1. Details of coalfield areas and coal measure rocks sample identity (ID).

State	Region	Mines	Type of mines	Sample ID
Jharkhand	Jharia coalfields	Ena colliery, Kusunda area	Open-cast	SST-1* SH-1*
		East Basuriya colliery, Kusunda area	Open-cast	SST-2 SH-2
		Katras area	Open-cast	SST-3 SH-3
		Mugma area**	Open-cast	SST-4
West Bengal	Raniganj coalfields	Damagoria, CV area***	Underground	SST-5 SH-4
		Amritnagar Satgram incline, Satgram area	Underground	SST-6 SH-5 SST-7 SH-6 SST-8 SH-7
		Amkula mines, Satgram area	Open-cast	SST-9 SST-10 SH-8
		Sonepur Bazari area	Open-cast	SST-11 SH-9 SST-12 SH-10 SST-13 SH-11
		Bankola area	Underground	SH-12
		Jhanjhra area	Underground	SST-14 SH-13

\*The abbreviation SST stands for sandstone, and SH stands for shale.

\*\*The Mugma coalfield area lies in the state of Jharkhand, but the area is under the authority of ECL.

\*\*\*The Damagoria coalfield area lies in the state of West Bengal, but the area is under the authority of BCCL.

and Ramakrishnan 2010). There are different river systems in India that resulted in the deposition of Lower Gondwana coal measure rocks: (i) Son–Narmada valley system; (ii) Mahanadi valley system; (iii) Damodar valley system, and (iv) Godavari valley system. The samples have been collected from the Raniganj Formation and Barakar Formation of Damuda Group of the Damodar River valley system. The Damodar River, shown in figure 1, flows from west to east and is located south of the location points.

### 3. Material and methods

The tests conducted in this paper are based on standards suggested by ISRM (International Society of Rock Mechanics) (1981a, b, c, d). In this study, dynamic (UPV), geomechanical (UCS and

BTS), and physical ( $\rho$  and  $\varphi$ ) tests have been used to analyse the behaviour of coal measure rocks under dry and saturated conditions. For dry testing, the specimens of sandstone and shale were dried in a dry-air oven at 105°C for 24 hours and for testing at saturation; the specimens were kept submerged in water for 24 hours (Dyke and Dobereiner 1991).

#### 3.1 Ultrasonic pulse velocity (UPV) test

The UPV tests have been conducted using the PROCEQ Pundit Lab instrument (Youash 1970; ISRM 1981a). Well-prepared rock specimens were used with flat polished ends (Core specimens) for good coupling with UPV transducers. The Pundit Lab instrument uses two transducers in which one is the transmitter and the other is the receiver. The transmitter converts the electrical energy into a

mechanical pulse, which travels through the specimen and reaches the receiver at the other end, which converts the mechanical pulse into electrical energy. When the length of the specimen is divided by the elapsed time of the ultrasonic pulse, it gives the velocity of the pulse (UPV).

### 3.2 Mechanical properties

UCS and BTS are the most commonly used geomechanical properties for any rock mass classification. These mechanical tests (UCS and BTS) were conducted based on ISRM (1981b, c, respectively) standards. To prepare the specimen for the test, rock samples of approximately 30 cm × 30 cm × 40 cm block size were collected from different colliery areas (figure 1 and table 1). These block samples were drilled (cored) to obtain 52 cm diameter core samples. These core samples were then cut and polished to give a flat cross-sectional surface to the cores. These specimens with a length to diameter ratio of ~2.5 for UCS and a thickness to diameter ratio of ~0.5 for the BTS test were prepared (figure 2). For the UCS test, the specimen is kept between the platens, and load at a constant rate is applied. The maximum

load at which the rock breaks is the strength of the rock. The UCS is calculated by the following equation:

$$UCS = \frac{P}{A}, \tag{1}$$

where  $P$  is load in N (Newton),  $A$  is cross-sectional area (mm<sup>2</sup>), and UCS is given in MPa.

BTS is an indirect method to determine the tensile strength of a rock. This method uses Brazilian jaws to instigate tensile stress in the rock (figure 2). The BTS for disc specimens were calculated by the following equation:

$$BTS = \frac{2P}{\pi LD}, \tag{2}$$

where  $P$  is load in N (Newton),  $D$  is the diameter (mm),  $L$  is the thickness (mm), and BTS is given in MPa.

### 3.3 Density and porosity

The saturation method was used to determine the intrinsic properties, i.e.,  $\rho$  and  $\phi$  of the specimens, in accordance with the standards of ISRM (1981d). The following equations were used to determine the dry density ( $\rho$ ) and effective porosity ( $\phi$ ),

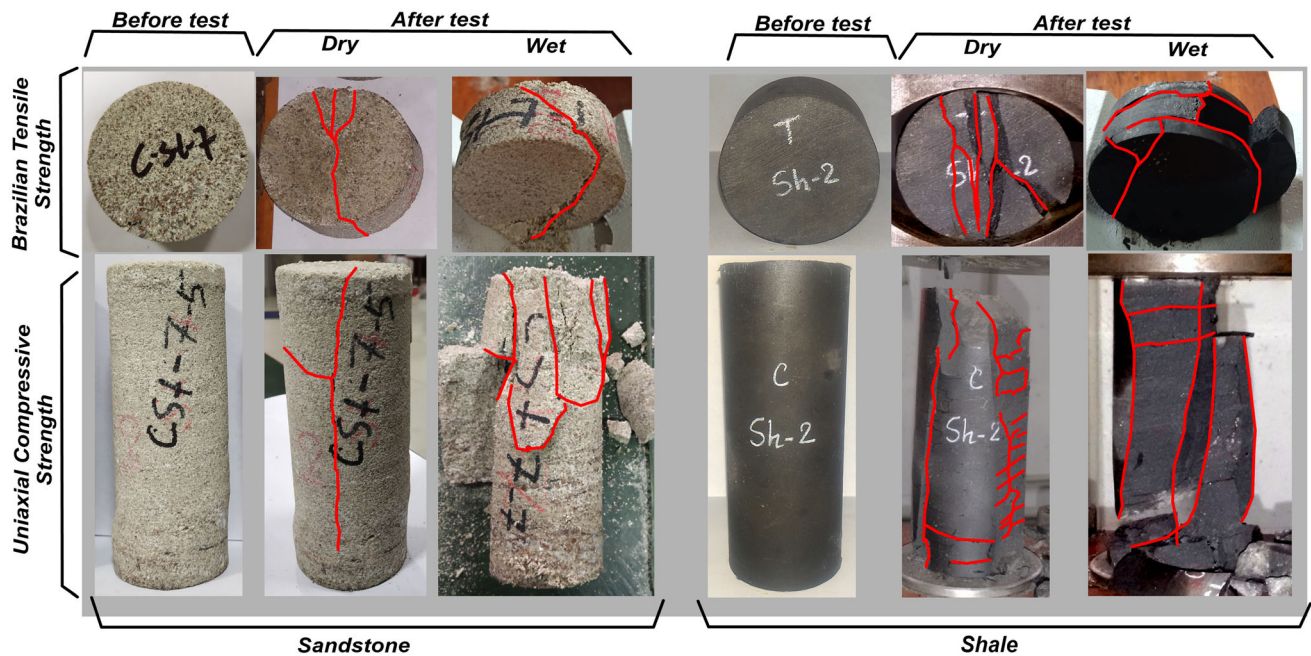


Figure 2. Breaking behaviour of sandstone and shale in dry and wet conditions.

respectively:

$$\rho = \frac{M_S}{V}, \quad (3)$$

$$\varphi = \frac{(M_{\text{sat}} - M_S)/\rho_w}{V} \times 100, \quad (4)$$

where  $M_S$  is the solid mass of the specimen,  $V$  is the bulk volume,  $M_{\text{sat}}$  is the saturated mass of the specimen, and  $\rho_w$  is the density of the water used.

## 4. Results

The sensitivity in the geomechanical properties and UPV of coal measure rocks have been discussed in this study. It was observed that the geomechanical properties of coal measure rocks reduced drastically when tested in saturated conditions as compared to in dry conditions. The change in UCS and BTS ( $\Delta_{\text{UCS}}$  and  $\Delta_{\text{BTS}}$ ) (equation 5) during testing in dry and saturated conditions has also been indicated in table 2. It was observed that the  $\Delta_{\text{UCS}}$  and  $\Delta_{\text{BTS}}$  were negative in all the cases indicating that the strength of the rock reduced when tested in the wet condition.

$$\Delta_X(\%) = \left( \frac{X_{\text{sat}} - X_{\text{dry}}}{X_{\text{dry}}} \right) \times 100, \quad (5)$$

where  $X$  is the geomechanical property (either UCS or BTS). The UPV measured in dry and saturated conditions are shown in table 2. It was observed that there is a marked increase in the UPV in the saturated condition as compared to the dry condition. The  $\Delta_{\text{UPV}}$  (equation 6) was observed to be positive in all the cases.

$$\Delta_{\text{UPV}}(\%) = \left( \frac{\text{UPV}_{\text{sat}} - \text{UPV}_{\text{dry}}}{\text{UPV}_{\text{dry}}} \right) \times 100. \quad (6)$$

## 5. Discussion

### 5.1 Simple regression analysis

In this paper, bivariate regression analysis has been performed, considering the best fit function to be linear ( $y = mx + c$ ), power ( $y = mx^c$ ), or exponential ( $y = me^x$ ). Where  $x$  is the independent variable,  $y$  is the dependent variable,  $m$  is the slope, and  $c$  is constant.

### 5.1.1 Correlation of geomechanical properties with the UPV

In order to predict the geomechanical properties of the rocks from the UPV, bivariate regression analysis has been used by different researchers (Kahraman and Yeken 2008; Khandelwal and Singh 2009; Abdi *et al.* 2018, etc.). Rahman *et al.* (2020) correlated UCS and BTS and dynamic elastic constants with the UPV of sandstones and shales of Lower Gondwana Formations of India. Khandelwal and Singh (2009) also proposed regressions to predict the UCS, BTS,  $\rho$ , shear strength, Poisson's ratio and Young's modulus using the UPV. Abdi *et al.* (2018) proposed empirical correlations between the mechanical properties and P-wave velocity for six different types of sandstones in different saturation conditions. In this study, sandstones and shales of Jharia and Raniganj coalfields were used to perform the geomechanical tests under dry and saturated conditions. Before geomechanical tests, all the specimens were used for non-destructive UPV tests under dry and saturated conditions. A total of 42 UCS (14 sets) and 42 BTS (14 sets) tests for sandstones and 39 UCS (13 sets) and 39 BTS (13 sets) tests for shale samples were conducted in dry and saturated conditions each. The correlations obtained between the geomechanical properties and UPV under dry and wet/saturated conditions for sandstones and shales have been shown in figure 3(a and b), respectively. It was observed that the regression obtained for shale samples showed a higher gradient than the regression of the sandstone samples (Rahman *et al.* 2020; Rahman and Sarkar 2021). The correlation equations obtained for sandstone samples are as follows:

$$\text{UCS}_{\text{dry}} = 8.7669e^{0.4421\text{UPV}_{\text{dry}}} (R^2 = 0.8238), \quad (7)$$

$$\text{UCS}_{\text{wet}} = 2.7475e^{0.6084\text{UPV}_{\text{wet}}} (R^2 = 0.7695), \quad (8)$$

$$\text{BTS}_{\text{dry}} = 0.5182 \times \text{UPV}_{\text{dry}}^{1.8791} (R^2 = 0.8315), \quad (9)$$

$$\text{BTS}_{\text{wet}} = 0.09 \times \text{UPV}_{\text{sat}}^{2.7689} (R^2 = 0.8309). \quad (10)$$

The change in geomechanical properties ( $\Delta_{\text{UCS}}$  and  $\Delta_{\text{BTS}}$ ) and  $\Delta_{\text{UPV}}$  from dry to saturated conditions are greater in the case of shale samples as compared to sandstone samples (figure 3b). The

Table 2. *The sensitivity of the geomechanical and UPV tests under the dry and saturated conditions for coal measure rocks.*

Sample ID	UPV <sub>dry</sub> (m/s)	UPV <sub>sat</sub> (m/s)	ΔUPV (%)	BTS <sub>dry</sub> (MPa)	BTS <sub>sat</sub> (MPa)	ΔBTS (%)	UCS <sub>dry</sub> (MPa)	UCS <sub>sat</sub> (MPa)	ΔUCS (%)	φ (%)	ρ (g/cm <sup>3</sup> )
SST-1	4.72	4.86	3.01	10.24	9.31	-9.08	79.18	55.32	-30.13	3.85	2.69
	4.60	4.72	2.72	9.23	7.33	-20.59	76.99	56.21	-26.99	2.88	2.66
	4.69	4.77	1.70	12.32	11.32	-8.12	77.28	51.23	-33.71	3.30	2.67
SST-2	3.48	3.76	7.98	7.25	5.68	-21.66	44.62	20.33	-54.44	3.39	2.55
	3.22	3.47	7.57	5.26	4.18	-20.53	36.55	19.63	-46.29	4.37	2.53
	3.40	3.65	7.50	6.80	4.12	-39.41	34.76	21.36	-38.55	3.38	2.53
SST-3	4.06	4.25	4.83	5.88	3.96	-32.65	48.78	33.54	-31.24	5.56	2.62
	3.85	4.17	8.15	5.18	3.66	-29.34	45.41	30.58	-32.66	5.54	2.62
	3.97	4.19	5.50	5.36	3.25	-39.37	46.39	28.36	-38.86	5.54	2.61
SST-4	2.67	3.04	13.84	3.54	1.88	-46.89	29.77	19.15	-35.67	9.77	2.29
	2.52	2.89	14.83	3.27	2.12	-35.17	25.98	18.62	-28.33	10.12	2.32
	2.54	2.74	7.80	3.38	2.12	-37.19	28.15	21.08	-25.10	9.89	2.31
SST-5	3.17	3.41	7.80	3.88	1.52	-60.82	25.31	16.92	-33.15	11.10	2.42
	2.96	3.35	13.20	4.78	2.38	-50.21	28.14	17.22	-38.81	10.55	2.40
	3.09	3.49	13.01	4.22	1.88	-55.45	27.97	15.20	-45.65	10.29	2.40
SST-6	4.32	4.52	4.60	5.68	4.12	-27.46	68.14	51.22	-24.83	3.66	2.61
	4.19	4.36	4.01	7.14	5.11	-28.43	64.68	55.64	-13.98	2.39	2.57
	4.27	4.49	5.32	6.65	4.23	-36.39	67.45	49.74	-26.26	3.38	2.59
SST-7	2.29	2.62	14.30	1.58	1.20	-24.05	14.31	8.41	-41.23	13.13	2.20
	2.06	2.41	17.41	1.98	1.10	-44.44	16.73	8.75	-47.70	13.98	2.14
	2.13	2.39	11.90	1.55	0.72	-53.43	15.92	8.39	-47.31	13.22	2.18
SST-8	3.32	3.66	10.11	7.44	4.21	-43.41	48.78	20.14	-58.71	7.88	2.38
	3.06	3.33	8.80	7.41	4.62	-37.65	46.51	19.78	-57.47	8.44	2.36
	3.19	3.52	10.22	7.08	3.37	-52.40	37.49	24.99	-33.36	8.51	2.39
SST-9	3.58	3.79	5.72	4.88	1.88	-61.48	31.44	22.58	-28.18	7.86	2.61
	3.22	3.66	13.57	5.76	2.12	-63.19	34.82	21.31	-38.80	9.66	2.55
	3.30	3.59	8.77	5.22	1.82	-65.07	33.09	24.61	-25.63	8.57	2.59
SST-10	3.96	4.15	5.01	7.22	6.41	-11.22	43.11	34.89	-19.07	6.19	2.61
	3.72	4.05	8.62	8.36	6.11	-26.91	48.84	33.27	-31.88	7.14	2.58
	3.80	4.05	6.42	8.36	6.90	-17.46	42.62	33.21	-22.08	6.23	2.62
SST-11	1.95	2.21	13.73	1.88	0.88	-53.19	24.72	14.15	-42.76	12.66	2.25
	1.75	2.04	16.93	1.29	0.65	-49.61	19.61	12.11	-38.25	14.12	2.22
	1.83	2.11	15.01	1.34	0.47	-65.10	22.82	11.76	-48.45	13.71	2.21
SST-12	3.94	4.05	2.79	3.84	3.34	-13.02	50.21	38.52	-23.28	2.55	2.51
	3.77	3.96	5.20	5.18	4.55	-12.16	44.55	36.12	-18.92	3.12	2.51
	3.81	4.03	5.82	4.13	3.74	-9.25	46.54	40.95	-12.03	2.97	2.49
SST-13	2.02	2.33	15.32	2.10	1.12	-46.67	22.52	14.22	-36.86	13.66	2.22
	1.71	2.02	18.22	1.88	0.88	-53.19	25.41	12.58	-50.49	14.55	2.20
	1.89	2.15	13.82	1.40	0.50	-64.26	23.44	3.78	-83.87	13.19	2.24
SST-14	2.25	2.56	13.35	1.88	1.25	-33.51	25.47	18.65	-26.78	10.98	2.18
	2.07	2.38	14.93	2.41	1.32	-45.23	27.54	17.88	-35.08	11.22	2.17
	2.20	2.48	13.19	2.19	1.20	-45.15	27.48	18.24	-33.64	12.92	2.19
SH-1	3.52	3.95	12.18	13.31	11.21	-15.78	78.64	58.46	-25.66	2.11	2.49
	3.38	3.99	18.12	14.42	10.55	-26.84	75.32	65.44	-13.12	2.87	2.51
	3.44	4.01	16.54	13.15	10.65	-19.01	73.24	71.32	-2.62	3.06	2.53
SH-2	3.02	3.38	11.85	9.48	4.81	-49.26	55.68	48.75	-12.45	4.41	2.46
	2.86	3.31	15.65	8.78	4.77	-45.67	58.12	42.38	-27.08	4.11	2.43
	2.98	3.34	12.08	8.56	4.28	-50.00	60.63	52.47	-13.46	4.94	2.43
SH-3	3.34	3.73	11.48	9.69	3.89	-59.86	65.32	42.81	-34.46	4.08	2.49
	3.19	3.58	12.13	7.61	3.22	-57.69	68.49	41.52	-39.38	4.47	2.44
	3.22	3.59	11.39	9.67	3.65	-62.30	62.64	44.58	-28.83	4.16	2.45

Table 2. (Continued.)

Sample ID	UPV <sub>dry</sub> (m/s)	UPV <sub>sat</sub> (m/s)	ΔUPV (%)	BTS <sub>dry</sub> (MPa)	BTS <sub>sat</sub> (MPa)	ΔBTS (%)	UCS <sub>dry</sub> (MPa)	UCS <sub>sat</sub> (MPa)	ΔUCS (%)	φ (%)	ρ (g/cm <sup>3</sup> )
SH-4	3.17	3.63	14.32	8.99	3.23	-64.07	71.28	28.66	-59.79	5.22	2.44
	2.91	3.29	12.91	7.63	3.42	-55.18	66.08	22.08	-66.59	5.84	2.43
	3.00	3.59	19.36	8.77	2.81	-67.99	67.94	24.56	-63.85	6.39	2.39
SH-5	2.76	3.16	14.70	8.52	4.53	-46.83	58.52	34.75	-40.62	2.66	2.45
	2.46	2.75	11.88	6.77	4.11	-39.29	56.06	34.22	-38.96	3.05	2.41
	2.59	2.82	8.78	7.27	3.56	-51.03	55.23	32.15	-41.79	2.06	2.47
SH-6	2.25	2.65	18.04	3.48	1.24	-64.37	34.68	7.80	-77.51	8.55	2.22
	1.96	2.27	15.93	2.39	0.88	-63.18	32.88	7.61	-76.86	7.14	2.26
	2.00	2.33	16.50	2.57	0.70	-72.76	31.79	6.90	-78.30	8.29	2.27
SH-7	2.49	2.96	18.94	7.53	1.25	-83.40	36.85	15.45	-58.07	9.65	2.34
	2.25	2.65	18.04	6.24	1.31	-79.01	41.22	18.53	-55.05	11.21	2.25
	2.39	2.79	16.33	6.80	0.89	-86.91	38.95	12.36	-68.27	9.55	2.32
SH-8	2.28	2.65	16.23	5.28	2.12	-59.85	33.54	15.41	-54.05	12.32	2.29
	2.19	2.61	19.18	6.88	1.98	-71.22	31.67	14.55	-54.06	11.85	2.28
	2.38	2.69	13.03	5.69	1.67	-70.65	32.18	16.38	-49.10	10.92	2.31
SH-9	2.76	3.10	12.33	6.11	3.25	-46.81	56.38	28.60	-49.27	8.79	2.38
	2.49	2.82	13.30	6.86	2.41	-64.87	51.25	26.33	-48.62	8.04	2.37
	2.61	3.07	17.29	6.56	1.16	-82.27	53.65	21.36	-60.19	8.20	2.35
SH-10	2.88	3.19	10.55	5.37	1.89	-64.80	36.10	18.88	-47.70	7.59	2.34
	2.64	3.01	13.99	4.52	1.47	-67.48	37.85	19.52	-48.43	6.81	2.33
	2.72	3.02	10.91	4.78	1.09	-77.23	38.00	18.28	-51.89	7.83	2.38
SH-11	2.98	3.44	15.59	6.62	2.14	-67.67	46.52	21.52	-53.74	10.76	2.31
	2.72	3.31	21.89	5.88	2.65	-54.93	45.21	23.12	-48.86	11.84	2.32
	2.81	3.31	17.99	5.75	2.23	-61.23	44.36	16.84	-62.04	10.35	2.32
SH-12	3.05	3.49	14.48	7.36	3.54	-51.90	46.85	34.58	-26.19	5.68	2.28
	2.86	3.26	13.81	9.21	2.87	-68.84	44.32	33.98	-23.33	5.88	2.31
	2.90	3.21	10.56	8.62	3.87	-55.10	46.32	28.61	-38.23	4.87	2.33
SH-13	3.23	3.65	13.02	8.22	5.22	-36.50	54.82	41.25	-24.75	6.55	2.41
	2.92	3.47	18.85	9.31	6.34	-31.90	55.36	39.56	-28.54	5.49	2.43
	3.14	3.68	17.38	8.41	6.39	-23.93	56.35	45.25	-19.70	6.75	2.40

correlation equations obtained for shale samples are as follows:

$$\text{UCS}_{\text{dry}} = 10.329e^{0.5622\text{UPV}_{\text{dry}}} (R^2 = 0.6764), \quad (11)$$

$$\text{UCS}_{\text{wet}} = 0.8354e^{1.0758\text{UPV}_{\text{wet}}} (R^2 = 0.6849), \quad (12)$$

$$\text{BTS}_{\text{dry}} = 0.8426 \times \text{UPV}_{\text{dry}}^{2.0933} (R^2 = 0.6631), \quad (13)$$

$$\text{BTS}_{\text{wet}} = 0.052e^{1.2459\text{UPV}_{\text{wet}}} (R^2 = 0.6371). \quad (14)$$

In figure 3(c), a comparison has been made between regressions obtained for shale and sandstone under dry and wet conditions and the previous study's database. Torok and Vasarhelyi (2010) suggested a regression to predict UCS from the UPV under the dry and wet conditions for Hungarian travertine rocks. The regression was observed to predict lower values of UCS for the corresponding UPV than the regression of

present study sandstones. Karakul and Ulusay (2013) proposed a general regression for multiple rock types, which agrees with the regression of the present study sandstones under dry and wet conditions. Rahman and Sarkar (2021) suggested a characteristic regression equation for particular lithology for 12 rock types, including shale and sandstone, which has also been compared in figure 3(c).

### 5.1.2 Correlation of UCS with the porosity and density

The effect of density and porosity on the relationship between the strength parameters of the rocks and UPV has been studied by different researchers (Kahraman and Yeken 2008; Vasconcelos *et al.* 2007, etc.). In the present study, 14 sets of tests for sandstone and 13 sets of tests for shale samples were performed, where, in each set three tests were conducted. The UCS has been correlated with the



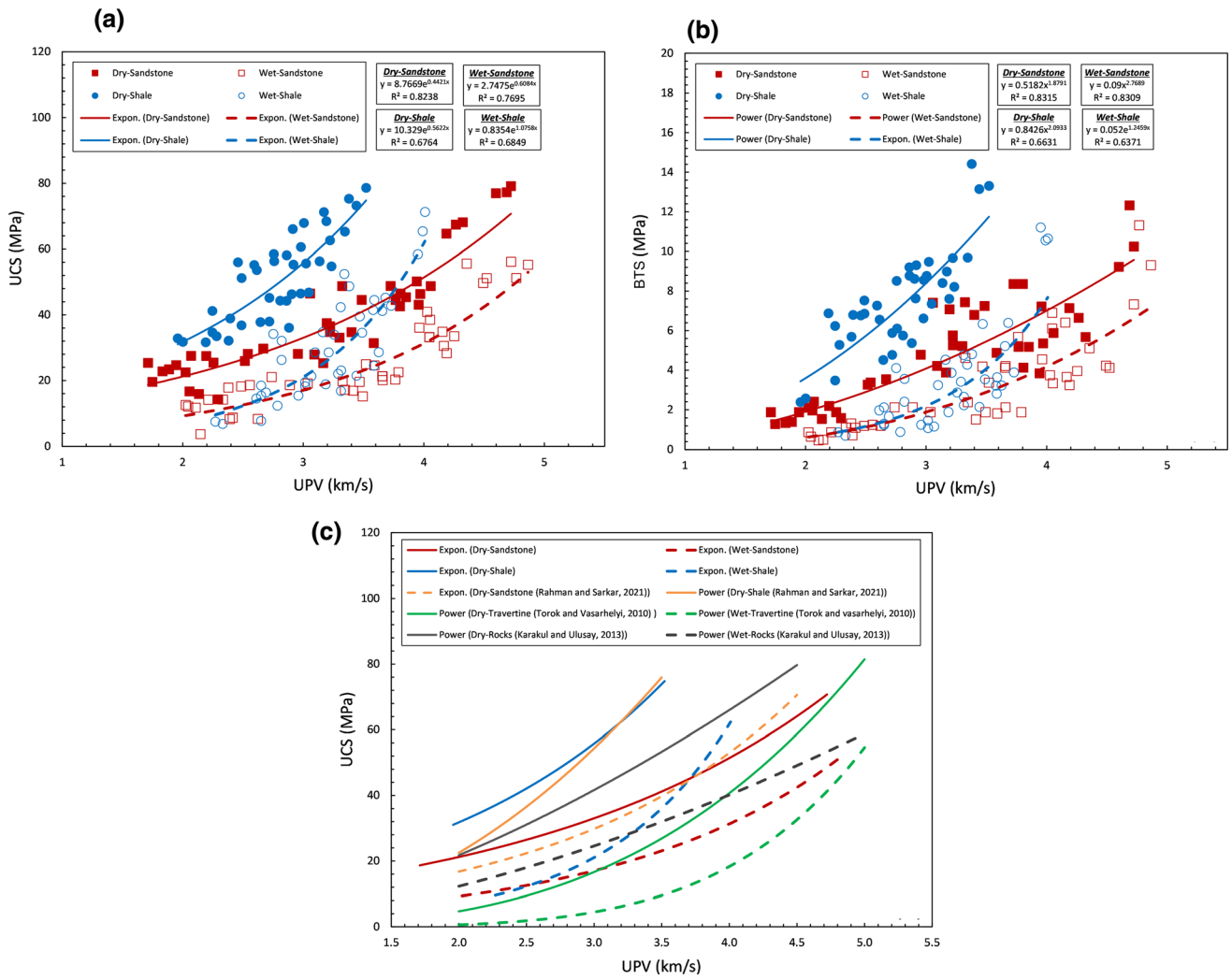


Figure 3. Relationship between UPV and (a) UCS, (b) BTS, and (c) comparative analysis with the previous studies for shale and sandstone samples.

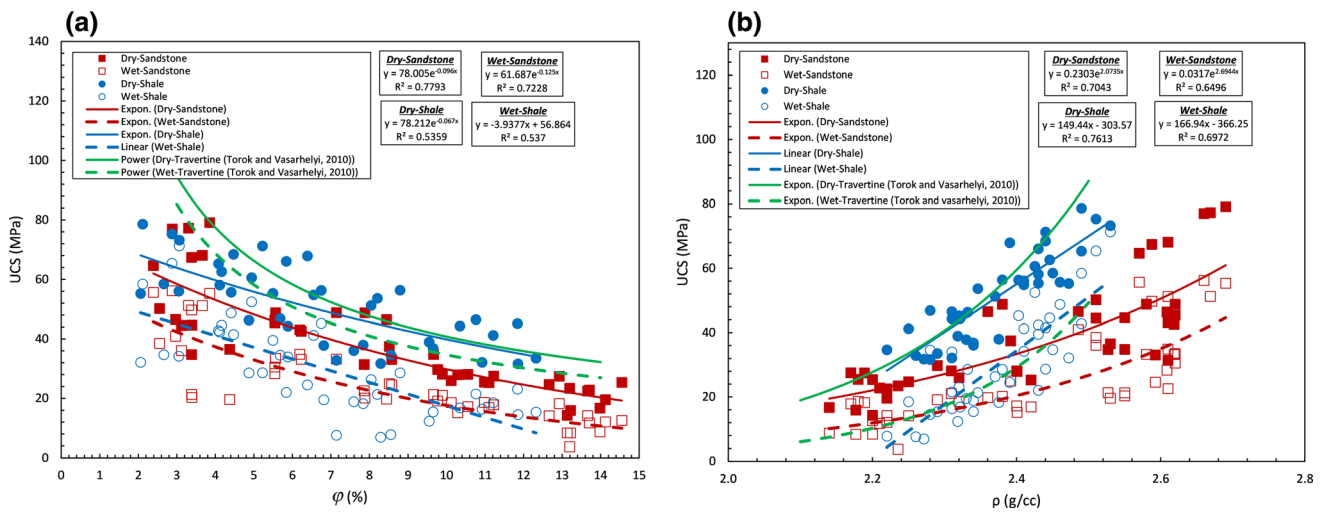


Figure 4. Relationship between (a) UCS and  $\phi$  and (b) UCS and  $\rho$  for sandstone and shale samples under dry and wet conditions.

$\varphi$  and  $\rho$  of both the rock types under study (figure 4a and b, respectively). It was observed that UCS has a negative correlation with the  $\varphi$  of the rock, meaning that the UCS decreases with an increase in the  $\varphi$  of the rock. The obtained regression equations are as follows:

For sandstone samples,

$$\text{UCS}_{\text{dry}} = 78.005e^{-0.096\varphi} (R^2 = 0.7793), \quad (15)$$

$$\text{UCS}_{\text{wet}} = 61.687e^{-0.125\varphi} (R^2 = 0.7228). \quad (16)$$

For shale samples,

$$\text{UCS}_{\text{dry}} = 78.212e^{-0.067\varphi} (R^2 = 0.5359), \quad (17)$$

$$\text{UCS}_{\text{wet}} = -3.9377\varphi + 56.864 (R^2 = 0.537). \quad (18)$$

Conversely, the UCS showed a positive correlation with the  $\rho$  of the rock, meaning that the strength of the rock increases with the increase in  $\rho$ . The observed regressions are as follows:

For sandstone samples,

$$\text{UCS}_{\text{dry}} = 0.2303e^{2.0735\rho} (R^2 = 0.7043), \quad (19)$$

$$\text{UCS}_{\text{wet}} = 0.0317e^{2.6944\rho} (R^2 = 0.6496). \quad (20)$$

For shale samples,

$$\text{UCS}_{\text{dry}} = 149.44\rho - 303.57 (R^2 = 0.7613), \quad (21)$$

$$\text{UCS}_{\text{wet}} = 166.94\rho - 366.25 (R^2 = 0.6972). \quad (22)$$

The obtained regressions have been compared with the previous study database. The regression proposed for travertine rocks by Torok and Vasarhelyi (2010) was observed to predict higher values of UCS than the regression proposed for sandstones in the present study. Torok and Vasarhelyi (2010) regressions for UCS and  $\rho$  coincide with the regressions obtained for shale samples (figure 4b).

### 5.1.3 Change in UPV, UCS and BTS with the $\rho$ and $\varphi$ under dry and saturated conditions

Ultrasonic waves can travel in solids, liquids and gases. The typical velocity of the ultrasonic wave in air is 330 and 1450 m/s in water. Hence, the  $\Delta_{\text{UPV}}$  from dry to saturated conditions for sandstones and shales were observed to be positive in all the cases. This trend of increase in UPV under saturated conditions can be regarded as a function of

water absorbed by the rock, which in turn depends on the intrinsic properties of the rocks. The relationship between the  $\Delta_{\text{UPV}}$  with  $\varphi$  and  $\rho$  for sandstone and shale samples has been shown in figure 5(a and b), respectively, where it was observed that the  $\Delta_{\text{UPV}}$  has a positive and negative relationship with the  $\varphi$  and  $\rho$ , respectively. The relationships have also been obtained between  $\Delta_{\text{UCS}}$  with  $\varphi$  and  $\rho$  (figure 5c and d, respectively) for sandstone and shale samples. The correlation between  $\Delta_{\text{UCS}}$  and  $\varphi$  shows a negative gradient, whereas the correlation between  $\Delta_{\text{UCS}}$  and  $\rho$  shows a positive gradient. The slope for shale has a steeper gradient indicating a greater  $\Delta_{\text{UCS}}$  with minor variation in intrinsic properties. Similarly, the relationship between  $\Delta_{\text{BTS}}$  and  $\varphi$  and  $\rho$  have been shown in figure 5(e and f), respectively.

### 5.1.4 Correlation between dry and saturated geomechanical properties

The sensitivity of rock is defined as the per cent (%) change in the strength of the geomechanical properties from dry to wet conditions. The sensitivity of the geomechanical properties of weaker rocks is higher than the sensitivity of strong rocks (Dyke and Dobereiner 1991). Similarly, the plotted data between  $\text{UCS}_{\text{dry}}$  and  $\text{UCS}_{\text{wet}}$  shows that the sensitivity of sandstone and shale samples is high for weak rocks, with weak shale samples showing greater sensitivity. On the other hand, Vasarhelyi (2003) database showed the sensitivity of all rock types (strong or weak) to be constant, as indicated in figure 6(a). Torok and Vasarhelyi (2010) also proposed a correlation between  $\text{UCS}_{\text{dry}}$  and  $\text{UCS}_{\text{wet}}$  for travertine rocks which shows the lowest sensitivity relatively. The regressions obtained between the  $\text{UCS}_{\text{dry}}$  and  $\text{UCS}_{\text{wet}}$  are as follows:

For sandstone samples,

$$\text{UCS}_{\text{wet}} = 0.7783\text{UCS}_{\text{dry}} - 4.4659 (R^2 = 0.8857). \quad (23)$$

For shale samples,

$$\text{UCS}_{\text{wet}} = 0.9488\text{UCS}_{\text{dry}} - 18.489 (R^2 = 0.6606). \quad (24)$$

The regression for  $\text{BTS}_{\text{dry}}$  vs.  $\text{BTS}_{\text{sat}}$  (figure 6b) has also been proposed as follows:

For sandstone samples,

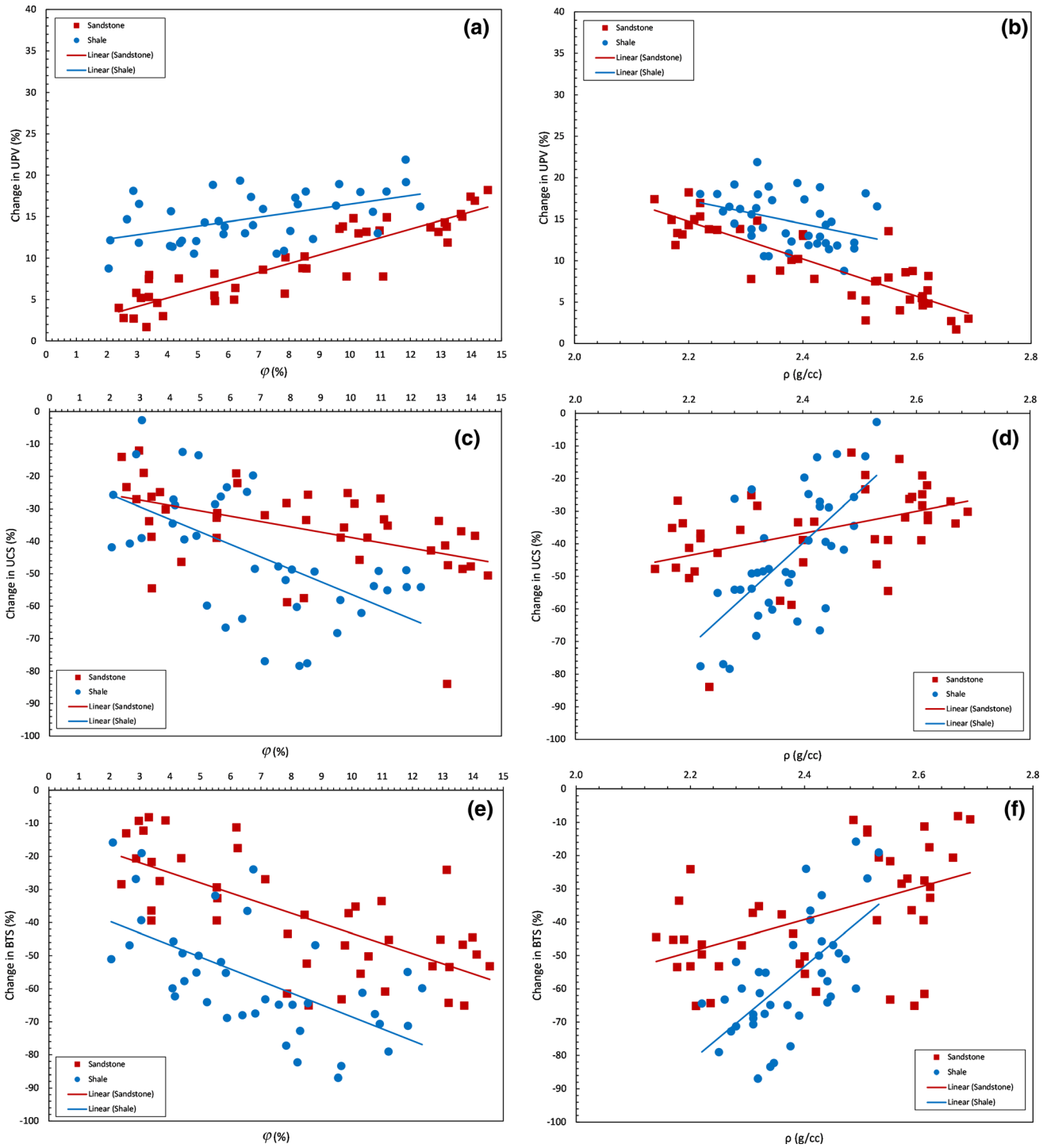


Figure 5. Relationship between change in UPV with (a)  $\phi$  and (b)  $\rho$ , change in UCS with (c)  $\phi$  and (d)  $\rho$ , and change in BTS with (e)  $\phi$  and (f)  $\rho$  for sandstone and shale samples.

$$BTS_{\text{wet}} = 0.8585BTS_{\text{dry}} - 0.9204 \quad (R^2 = 0.8812). \quad (25)$$

For shale samples,

$$BTS_{\text{sat}} = 0.8736BTS_{\text{dry}} - 3.0455 \quad (R^2 = 0.7571). \quad (26)$$

### 5.1.5 Correlation between dry and saturated UPV

Kahraman (2007) proposed a strong correlation between dry and wet UPV for sedimentary, metamorphic and igneous rocks. The equation for sedimentary rocks has been used in figure 7. In the present

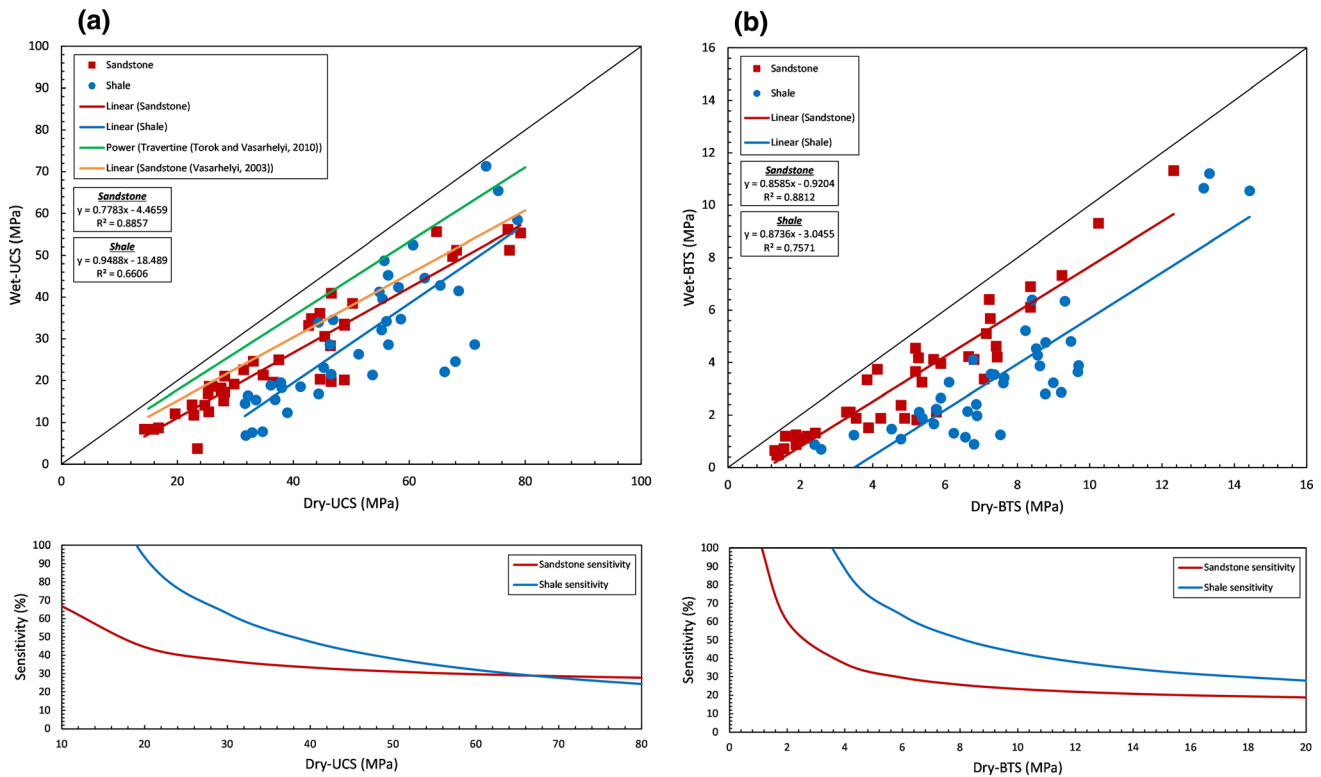


Figure 6. Relationship between (a)  $UCS_{dry}$  and  $UCS_{wet}$  and (b)  $BTS_{dry}$  and  $BTS_{wet}$ .

study, the relationship between  $UPV_{dry}$  and  $UPV_{sat}$  of coal measure rocks (sandstone and shale) was found to have a strong correlation with an excellent  $R^2$  value (figure 7). The correlation equations obtained are as follows:

For sandstone samples,

$$UPV_{wet} = 0.9476UPV_{dry} + 0.4306 \quad (R^2 = 0.9943). \quad (27)$$

For shale samples,

$$UPV_{wet} = 1.0972UPV_{dry} + 0.1387 \quad (R^2 = 0.9643). \quad (28)$$

Torok and Vasarhelyi (2010) regression for travertine rocks crosscut the regression of Kahraman (2007) for sedimentary rocks. Vasconcelos *et al.* (2007) suggested a similar correlation for granite rocks which predicts much higher values than other regressions shown. The present study linear regression lies closer to the 1:1 line than any other previous study regressions.

### 5.2 Multivariate regression analysis

Multivariate regression (MR) analysis was first used by Pearson in 1908. It is a robust tool to

analyse multiple independent variables to achieve a single dependent variable. The general MR equation is of the form;  $y = c + a_1x_1 + a_2x_2 + \dots + a_nx_n$ , where  $c$  is the constant,  $a_1, a_2, \dots, a_n$  are regression coefficients,  $x_1, x_2, \dots, x_n$  are independent variables, and  $y$  is the dependent variable. In nature, any phenomenon is a function of the interaction between multiple elements. Similarly, in geoscience and rock mechanics, the mechanical index property of a rock, such as UCS, is related to numerous other rock properties, such as the UPV,  $\phi$  and  $\rho$ , as we have observed in the simple regression analysis section.

In this paper, our aim is to estimate the change in the strength parameters and dynamic behaviour of sandstone and shale rocks which are associated with the mining operations of coal in the Jharia and Raniganj coalfields of Jharkhand and West Bengal, respectively. Here, we have used the multivariate regression analysis to estimate the UCS, BTS and UPV in wet conditions using their corresponding values in dry conditions, intrinsic properties ( $\phi$  and  $\rho$ ) and the rock type information (table 3). The rock type information was indexed as 1 for sandstone and 2 for shale.

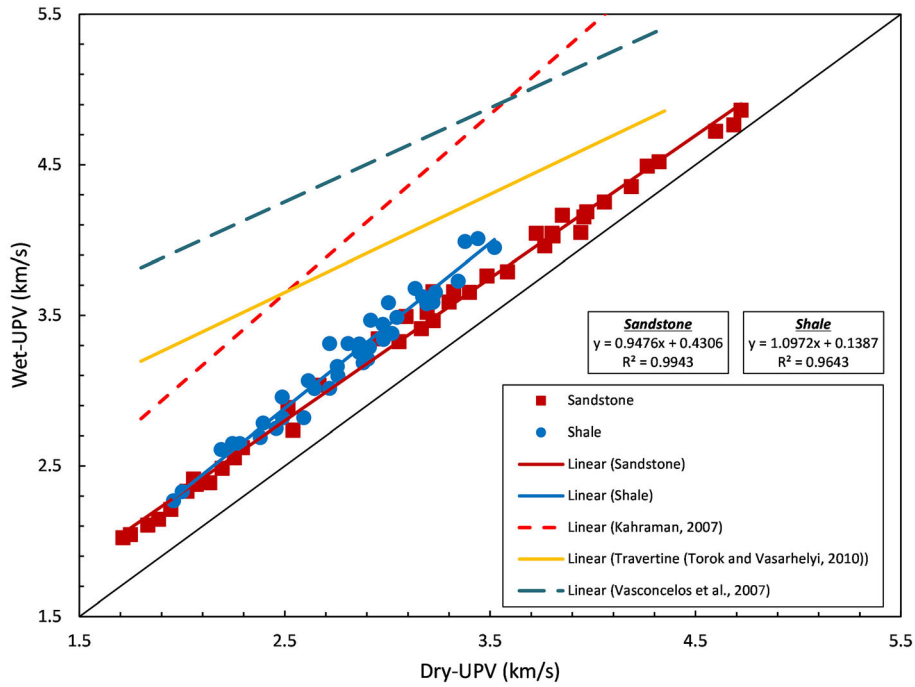


Figure 7. Relationship between  $UPV_{dry}$  and  $UPV_{wet}$ .

Table 3. Coefficients obtained for different parameters in saturated conditions using multivariate regression analysis.

Input parameters ( $x$ )	Coefficients		
	$UCS_{dry}$ (MPa)	$UPV_{dry}$ (km/s)	$BTS_{dry}$ (MPa)
Intercept	10.53557	-0.05461	8.62477
$X_1^*$	0.66828	1.02236	0.81371
$\varphi$ (%)	-0.91389	0.01208	-0.15714
$\rho$ (g/cm <sup>3</sup> )	0.80867	-0.00820	-2.38226
Rock type	-5.18123	0.16980	-2.24898

\* $X_1$  = Corresponding input parameter in dry conditions, respectively.

### 5.3 Artificial neural network

Artificial neural network (ANN) is an artificial modelling technique that mimics the function of a biological brain. The biological brain consists of numerous connections of neurons that generate (an output) specific information with certain association of neurons. Similarly, ANN consists of nodes and connections of weights that are analogous to neurons and connections of neurons of the brain. The main components of a network are a set of the input layer, a set of hidden layers (one or more) and a set of the output layer. The processing of the information takes place in the hidden layers. Each input parameter ( $x$ ) interact with the hidden layers by an

appropriate weight ( $W$ ) and bias ( $b$ ) based on the output parameter ( $y$ ). The weighted signal ( $Wx$ ) at each node is collected and added as the weighted sum. The mathematical representation of the interaction between the input and output layers is as follows:

$$y = W_0 + \sum_{j=1}^m W_j g \left( W_{0j} + \sum_{i=1}^n W_{ij} x_i \right) + b_i, \quad (29)$$

where  $i = 1, 2, 3, \dots, n$  and  $j = 1, 2, 3, \dots, m$ ,  $n$  is the number of input nodes and  $m$  is the number of hidden nodes,  $g$  is the activation function which is a sigmoidal function.

In the present study, the multi-layer perceptron method was employed, which is considered one of

the best ANN methods. The method consists of a three-layer system of nodes (Input–Hidden–Output). The network was trained using a Bayesian Regularisation training algorithm ('trainbr'

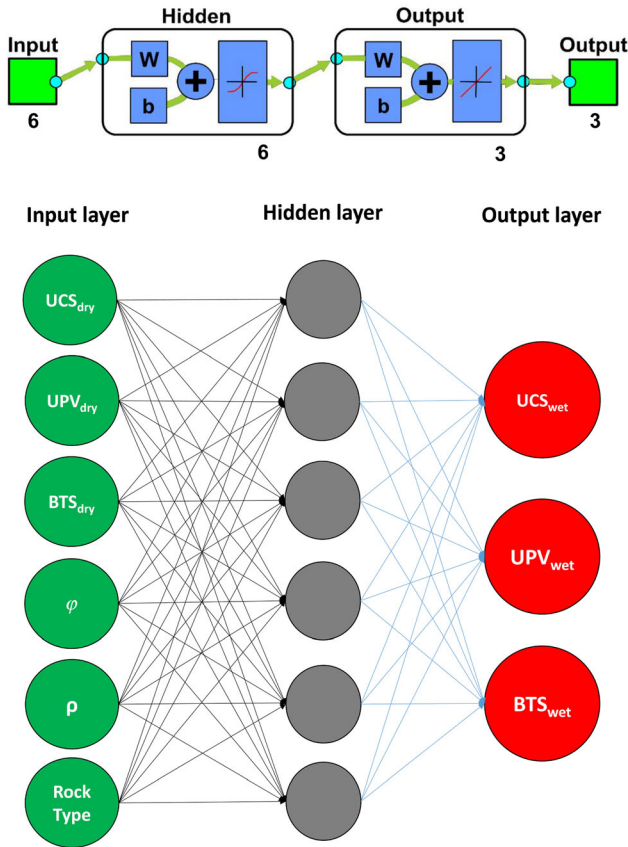


Figure 8. The neural structure of the developed ANN model.

function) in MATLAB using the Neural Fitting app. Six sets of input parameters ( $UPV_{dry}$ ,  $BTS_{dry}$ ,  $UCS_{dry}$ ,  $\rho$ ,  $\phi$  and rock type) and three sets of output parameters ( $UCS_{wet}$ ,  $UPV_{wet}$  and  $BTS_{wet}$ ) were fed to the network for training purposes. It means when the network is trained, it will generate three output parameters by providing six input parameters  $\{y = net(x)\}$  (figure 8). When the number of hidden layer is one, it is called shallow neural network (SNN), and when it is more than one, then the network is called a deep neural network (DNN). In the hidden and output layer, the network comprises the logarithmic sigmoidal function and the sigmoidal tangent function, respectively.

In this paper, a total of 81 datasets (42 sandstones and 39 shales) were used to develop an ANN model such that 69 datasets (85%) were used to train the network, and 12 datasets (15%) were used for testing of the developed ANN model. The ANN validation curve shows that the best training performance of 2.8875 occurred at epoch 201 (figure 9a). The regression plot for training, testing and overall dataset for the developed model has been shown in figure 9(b).

#### 5.4 Comparative analysis

The ANN model was developed to predict strength parameters in wet conditions using UCS, UPV,

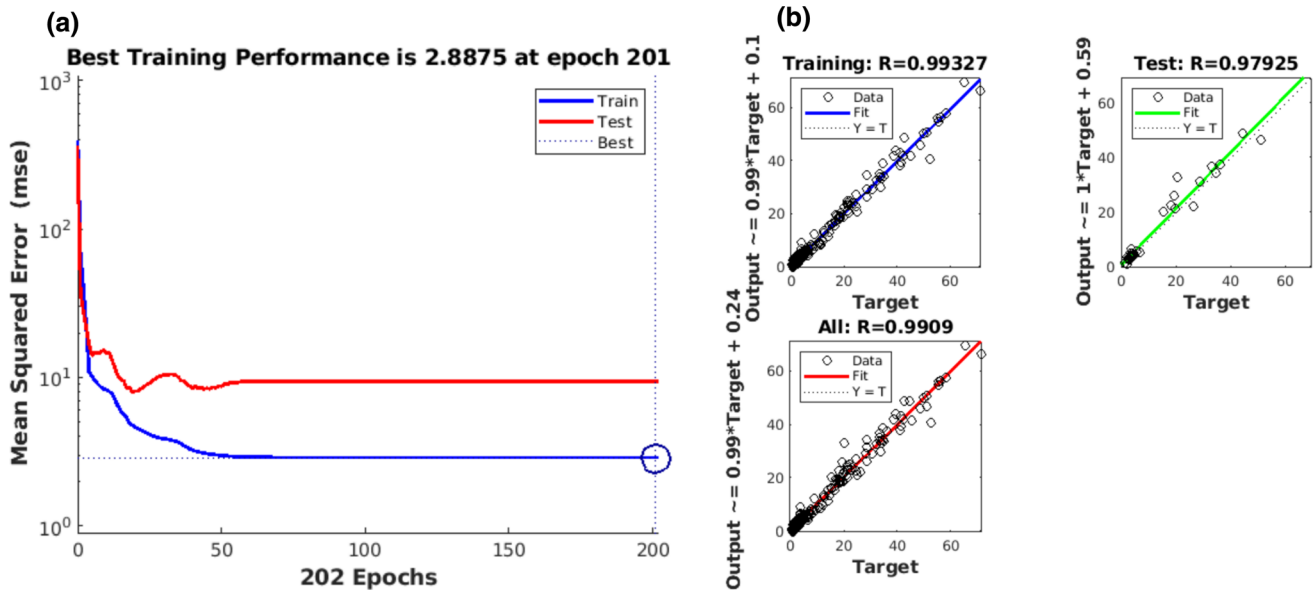


Figure 9. Showing the best training performance of the ANN model (a), and the obtained regression of the ANN model (b).

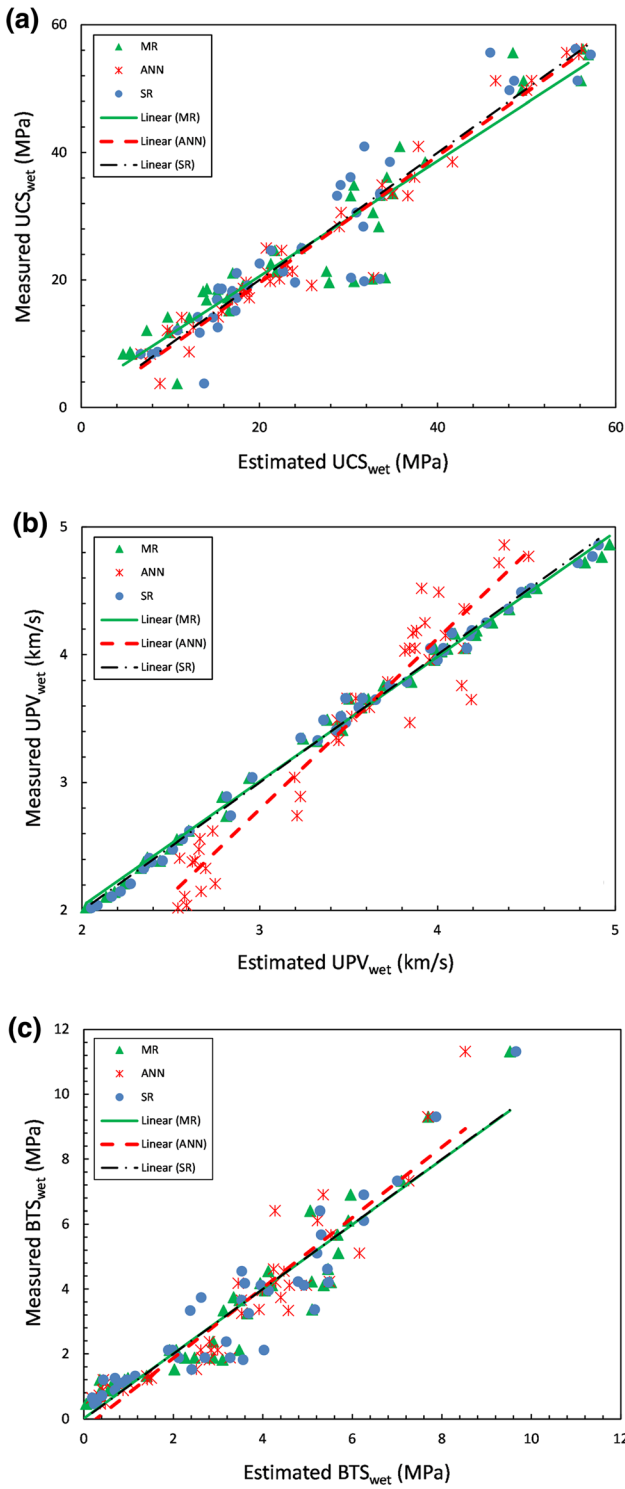


Figure 10. Measured *vs.* estimated plots for (a) UCS, (b) UPV and (c) BTS in wet/saturated condition for sandstone samples.

BTS in a dry condition,  $\rho$ ,  $\phi$ , and rock type information. Since the trends of the regressions to predict UCS from UPV for shale and sandstone are different, the coefficient of correlation ( $R = 0.99327$ ) values obtained during the training of the network are exceptional. A comparative

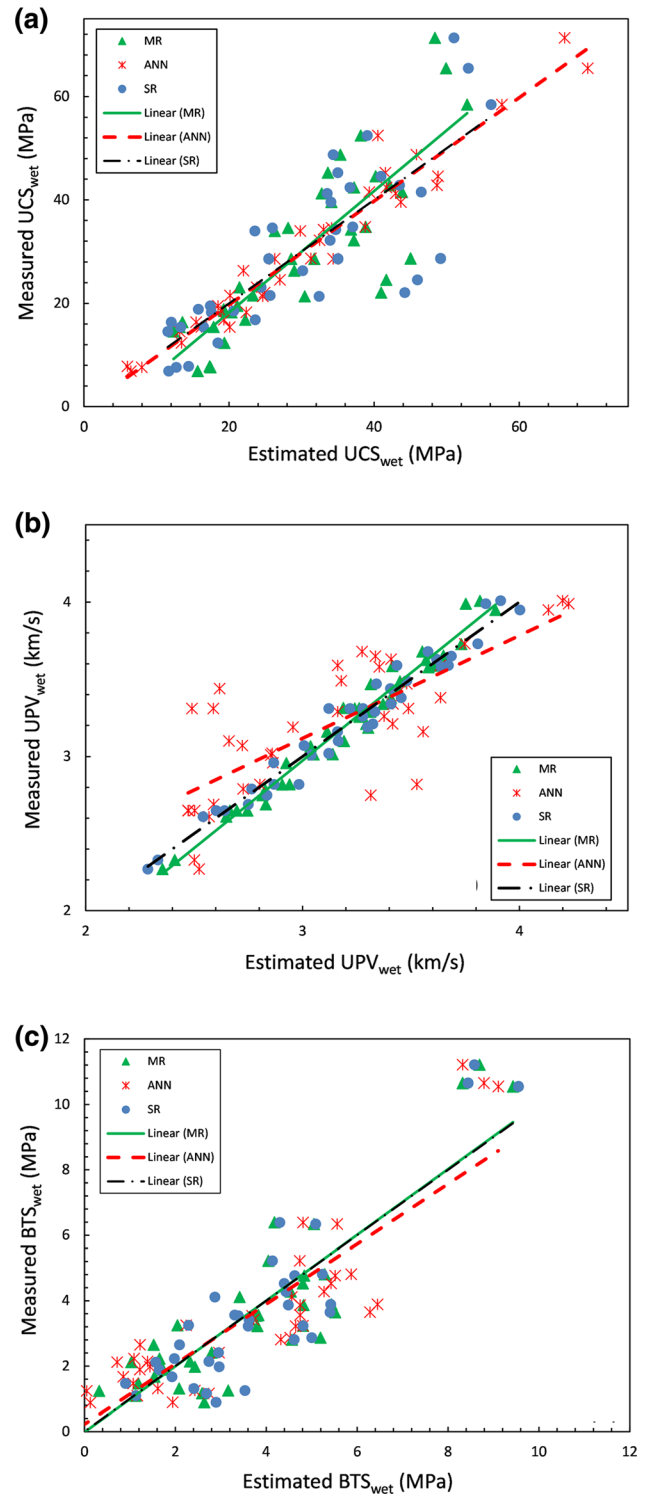


Figure 11. Measured *vs.* estimated plots for (a) UCS, (b) UPV and (c) BTS in wet/saturated condition for shale samples.

analysis between the measured and predicted values using SR, MR and ANN models is shown in figures 10 and 11 for sandstone and shale, respectively. In the 1:1 ( $x:y$ ) scatter plot, it was observed that the predicted values from SR, MR and ANN model lie close to each other and the 1:1 line.

Table 4. Statistical performance of the used MR, ANN, and SR models.

Predicted parameters	Statistical parameters	MR		ANN		SR	
		Sandstone	Shale	Sandstone	Shale	Sandstone	Shale
UCS <sub>wet</sub>	RMSE	4.8136	8.7979	2.9500	3.4595	4.7495	9.0889
	MAPE	2.8008	1.9197	3.2136	2.2673	3.0044	2.2800
	$R^2$	0.89	0.70	0.96	0.95	0.8857	0.6606
UPV <sub>wet</sub>	RMSE	0.0662	0.0908	0.3166	0.3364	0.0641	0.0823
	MAPE	1.7582	18.4169	16.5437	13.8654	20.0542	16.1652
	$R^2$	0.99	0.97	0.92	0.58	0.9942	0.9646
BTS <sub>wet</sub>	RMSE	0.7784	1.2211	0.8911	1.2679	0.8379	1.2571
	MAPE	26.7868	17.5363	21.3305	24.7902	18.5207	23.2702
	$R^2$	0.90	0.77	0.87	0.76	0.8812	0.7572

Hence, the predicted values using the SR, MR and ANN models are statistically acceptable. The ANN model can predict multiple output parameters, while MR and SR models can only predict a single output parameter. Moreover, MR can incorporate multiple input (independent variable) parameters for better generalisation of the dataset, while SR uses only one independent variable for the prediction of the dependent variable.

Statistical parameters such as coefficient of determination ( $R^2$ ), root mean square error (RMSE) and mean absolute percentage error (MAPE) have been used to evaluate the statistical performance of the proposed models. The closer the value of  $R^2$  to 1.0, the better the model, while the smaller the values of MAPE and RMSE, the better the model (table 4).

$$\text{RMSE} = \sqrt{\frac{1}{n} \sum_{i=1}^n (M_i - P_i)^2}, \quad (30)$$

$$\text{MAPE} = \frac{1}{n} \sum_{i=1}^n \left\{ \frac{|M_i - P_i|}{M_i} \times 100 \right\}, \quad (31)$$

where  $M_i$  is the measured  $i$ th value,  $P_i$  is the  $i$ th predicted value, and  $n$  is the total number of iterations.

## 6. Summary and conclusions

This paper was aimed to study the changes in strength behaviour under dry and water-saturated conditions of Lower Gondwana coal measure rocks of India. It was observed that the strength parameters reduced while the UPV increased when tested in a saturated condition relative to dry conditions. Empirical correlations were proposed between strength parameters and UPV for shales

and sandstones under dry and saturated conditions. The obtained positive regression trends for shales have a steeper gradient than the regressions obtained for sandstones.

Positive correlations have been established between dry and saturated UCS and  $\rho$ , while negative correlations were established between dry and saturated UCS and  $\phi$  for sandstone and shale rocks. The correlation between  $\Delta_{\text{UPV}}-\rho$  and  $\Delta_{\text{UPV}}-\phi$  showed a negative and positive trend, respectively, for coal measure rocks. Similarly, changes in UCS and BTS have been observed to have a negative correlation with the  $\phi$ , while it shows a positive correlation with the  $\rho$  of sandstone and shale samples.

Regressions to predict the strength parameters in saturated conditions from strength parameters in dry conditions have also been established. The correlation suggests that the change in strength parameters from dry to saturated condition is greater in weak samples than in strong samples. Similarly, relationship between  $\text{UPV}_{\text{dry}}-\text{UPV}_{\text{wet}}$  has also been proposed for coal measure rocks.

Finally, ANN, SR and MR models were used to predict strength parameters and UPV under saturated condition for coal measure rocks. The predicted values using ANN, SR and MR models were plotted in a 1:1 scatter plot against corresponding measured values and compared. ANN model was considered best, as it has the highest generalisation capacity of the dataset and predicts multiple output parameters.

The study presents empirical equations to predict the UCS, BTS and UPV in saturated conditions using the geomechanical, physical and dynamic properties in the dry conditions for sandstone and shale rocks of Lower Gondwana. The obtained regressions were compared with the regressions obtained in the previous studies, and a



clear lithological control in the regressions was observed. The lithological control can also be seen between the regressions of sandstone and shale samples used in the present study. Therefore, it can be suggested that the regressions proposed for a particular rock type can only be used for that rock type only.

## Acknowledgements

The authors acknowledge the resources provided by the Indian Institute of Technology (Indian School of Mines) Dhanbad. They are also thankful to the Eastern Coalfields Ltd. and Bharat Coking Coal Ltd. authorities for their support and guidance during the sample collection process.

## Author statement

Tabish Rahman: Conceptualisation, methodology, writing – original draft preparation, formal analysis, and visualisation. Kripamoy Sarkar: Writing – reviewing and validation.

## References

- Abdi Y, Khanlari G R and Jamshidi A 2018 Correlation between mechanical properties of sandstones and P-wave velocity in different degrees of saturation; *Geotech. Geol. Eng.* **10** 1–10.
- Altindag R 2012 Correlation between P-wave velocity and some mechanical properties for sedimentary rocks; *J. South. Afr. Inst. Min. Metall.* **112** 229–237.
- Azimian A 2017 Application of statistical methods for predicting uniaxial compressive strength of limestone rocks; *Acta Geotech.* **12** 321–333.
- Chary K B, Sarma L P and Lakshmi K J P 2006 Evaluation of engineering properties of rock using ultrasonic pulse velocity and uniaxial compressive strength; *Proc. Natl. Semin.* 379–385.
- Dyke C G and Dobereiner L 1991 Evaluating the strength and deformability of sandstones; *Quart. Eng. Geol.* **24** 123–134.
- Fox C S 1930 The Jharia coalfield; *Geol. Surv. India Memoir* **56** 255.
- Geological Survey of India (GSI) 2003 Coal resources of West Bengal (ed.) Dutta A B, *Bull. Geol. Surv. Ind. Ser. A* **45** 1–109.
- Ghabousi J, Garret Jr J H and Wu X 1991 Knowledge-based modelling of material behaviour with neural networks; *J. Eng. Mech. ASCE* **117**(1) 132–153.
- Hawkins A B and McConnell B J 1992 Sensitivity of sandstone strength and deformability to changes in moisture content; *Quart. Eng. Geol.* **25** 115–130.
- International Society of Rock Mechanics (ISRM) 1981a Suggested method for rock characterisation, testing and monitoring; In: *ISRM Commission on Testing Methods* (ed.) Brown E T, Pergamon Press, Oxford, pp. 107–110.
- International Society of Rock Mechanics (ISRM) 1981b Suggested method for rock characterisation, testing and monitoring; In: *ISRM Commission on Testing Methods* (ed.) Brown E T, Pergamon Press, Oxford, pp. 113–114.
- International Society of Rock Mechanics (ISRM) 1981c Suggested method for rock characterisation, testing and monitoring; In: *ISRM Commission on Testing Methods* (ed.) Brown E T, Pergamon Press, Oxford, pp. 119–121.
- International Society of Rock Mechanics (ISRM) 1981d Suggested method for rock characterisation, testing and monitoring; In: *ISRM Commission on Testing Methods* (ed.) Brown E T, Pergamon Press, Oxford, pp. 84–85.
- Kahraman S 2007 The correlations between the saturated and dry P-wave velocity of rocks; *Ultrasonics* **46** 341–348.
- Kahraman S and Yeken T 2008 Determination of physical properties of carbonate rocks from P-wave velocity; *Bull. Eng. Geol. Environ.* **67** 277–281.
- Karakul H and Ulusay R 2013 Empirical correlations for predicting strength properties of rocks from P-wave velocity under different degrees of saturation; *Rock Mech. Rock Eng.* **46** 981–999.
- Khandelwal M and Singh T N 2009 Correlating static properties of coal measures rocks with P-wave velocity; *Int. J. Coal Geol.* **79** 55–60.
- Kilic A and Teymen A 2008 Determination of mechanical properties of rocks using simple methods; *Bull. Eng. Geol. Environ.* **67** 237–244.
- Lin M L, Jeng F S, Tsai L S and Huang T H 2005 Wetting weakening of tertiary sandstones – microscopic mechanism; *Environ. Geol.* **48** 265–275.
- Mashinskii E I 2009 Strain amplitude-dependent attenuation of P and S waves in dry and water-saturated sandstone under confining pressure; *Russian Geol. Geophys.* **50** 734–738.
- Rahman T and Sarkar K 2021 Lithological control on the estimation of uniaxial compressive strength by the P-wave velocity using supervised and unsupervised learning; *Rock Mech. Rock Eng.* **54** 3175–3191.
- Rahman T, Sarkar K and Singh A K 2020 Correlation of geomechanical and dynamic elastic properties with the P-wave velocity of Lower Gondwana coal measure rocks of India; *Int. J. Geomech.* **20**(10) 04020189.
- Sharma P K and Singh T N 2008 A correlation between P-wave velocity, impact strength index, slake durability index and uniaxial compressive strength; *Bull. Eng. Geol. Environ.* **67** 17–22.
- Singh V K, Singh D and Singh T N 2001 Prediction of strength properties of some schistose rocks from petrographic properties using artificial neural networks; *Int. J. Rock Mech. Min. Sci.* **38** 269–284.
- Sharma L K, Vishal V and Singh T N 2017 Developing novel models using neural networks and fuzzy systems for the prediction of strength of rocks from key geomechanical properties; *Measurement* **102** 158–169.
- Steiger R P and Leung P K 1990 Lecture: Predictions of wellbore stability in shale formations at great depth; In: *Eurock (Rock at great depth)* (eds) Maurý et Fourmaintraux, Balkema, pp. 1209–1218.
- Torok A and Vasarhelyi B 2010 The influence of fabric and water content on selected rock mechanical parameters of travertine, examples from Hungary; *Eng. Geol.* **115** 237–245.

Vaidyanadhan R and Ramakrishnan M 2010 Geology of India; *Geol. Soc. India* **2** 615–661.

Vasarhelyi B 2003 Some observations regarding the strength and deformability of sandstones in case of dry and saturated conditions; *Bull. Eng. Geol. Environ.* **84** 70–74.

Vasconcelos G, Lourenco P B, Alves C S A and Pamplona J 2007 Prediction of the mechanical properties of granites by ultrasonic pulse velocity and Schmidt hammer hardness;

*North American Masonry Conference, Missouri, 3–5 June. The Masonry Society, CO*, pp. 980–991.

Yasar E and Erdogan Y 2004 Correlating sound velocity with the density, compressive strength and Young's modulus of carbonate rocks; *Int. J. Rock Mech. Min. Sci.* **41** 871–875.

Youash Y Y 1970 Dynamic physical properties of rocks: Part II, experimental results; *Int. Soc. Rock Mech. Proc.: 2<sup>nd</sup> Congr. Int. Soc. Rock Mech., Beograd* **1** 185–195.

Corresponding editor: SAIBAL GUPTA